

# Comparative Assessment of Empirical Coke Deposition Models during n-Butanol Dehydration over a Zeolite-Y-Based Cracking Catalyst

Tri Partono Adhi<sup>1</sup>, Subagio<sup>1,2</sup>, IGBN Makertihartha<sup>1,2</sup>, Azizah Nabilah<sup>2</sup>, Hanief Aulia<sup>2</sup>,  
Melia Laniwati Gunawan<sup>1,2\*</sup>

<sup>1</sup>Catalysis and Process System Research Group, Faculty of Industrial Technology, Institut Teknologi Bandung,  
Jl. Ganesha No. 10, Labtek X, Bandung 40132, West Java, Indonesia.

<sup>2</sup>Center for Catalysis and Reaction Engineering, Institut Teknologi Bandung, Jl. Ganesha No. 10, Labtek X,  
Bandung 40132, West Java, Indonesia.

Received: 27<sup>th</sup> December 2025; Revised: 22<sup>th</sup> February 2026; Accepted: 23<sup>th</sup> February 2026  
Available online: 1<sup>st</sup> March 2026; Published regularly: August 2026



## Abstract

The dehydration of *n*-butanol to butenes over zeolite-Y is accompanied by coke formation, which progressively deactivates the catalyst and affects reaction kinetics. In this study, dehydration was performed in an isothermal fixed-bed reactor at 400–500 °C using a commercial zeolite-Y composite catalyst. Coke deposition was quantified gravimetrically, while catalyst characterization showed a Si/Al ratio of 6, surface area of 353.9 m<sup>2</sup>.g<sup>-1</sup>, pore diameter of 57.2 Å, and pore volume of 0.602 cm<sup>3</sup>.g<sup>-1</sup>, confirming a mesoporous structure. Coke accumulation data were analyzed using the Voorhies power-law model and analytical expressions derived from the Dumez–Froment empirical model. Model parameters were estimated by fitting experimental coke content data at different temperatures. The Voorhies model showed excellent agreement with experimental data ( $R^2 = 0.96–0.98$ ). Among the Dumez–Froment-based expressions, only the logarithmic form accurately described coke deposition, while other forms resulted in poor fits. The results indicate that coke formation is progressively inhibited by accumulated coke, likely due to pore blockage and reduced accessibility of active sites. These findings identify suitable empirical models for predicting coke deposition and catalyst deactivation during *n*-butanol dehydration over zeolite-Y catalysts.

Copyright © 2026 by Authors, Published by BCREC Publishing Group. This is an open access article under the CC BY-SA License (<https://creativecommons.org/licenses/by-sa/4.0>).

**Keywords:** Coke deposit; modeling of coke deposit; cracking catalyst; n-butanol dehydration; Y-zeolite

**How to Cite:** Adhi, T. P., Subagio, S., Makertihartha, I. G. B. N., Nabilah, A., Aulia, H., Gunawan, M. L. (2026). Comparative Assessment of Empirical Coke Deposition Models during n-Butanol Dehydration over a Zeolite-Y-Based Cracking Catalyst. *Bulletin of Chemical Reaction Engineering & Catalysis*, 21 (2), 428-440. (DOI: 10.9767/bcrec.20612)

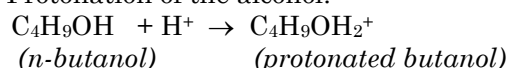
**Permalink/DOI:** <https://doi.org/10.9767/bcrec.20612>

## 1. Introduction

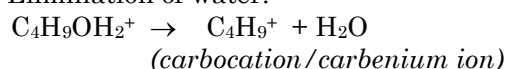
The dehydration of butanol (C<sub>4</sub>H<sub>9</sub>OH) to produce butene (C<sub>4</sub>H<sub>8</sub>) is a crucial chemical process in industrial chemistry, especially in the synthesis of various chemicals and fuels. This reaction involves an elimination process wherein a water molecule (H<sub>2</sub>O) is removed from butanol, a four-carbon alcohol, leading to the formation of butene, a four-carbon alkene [1,2]. The process uses acid catalysts, such as sulfuric acid (H<sub>2</sub>SO<sub>4</sub>)

or phosphoric acid (H<sub>3</sub>PO<sub>4</sub>), which provide protons to associate with the hydroxyl group (-OH) of the butanol molecule, resulting in carbocation formation, thereby facilitating the detachment of the hydroxyl group to generate water molecules [3]. The subsequent elucidation pertains to the mechanism of butanol dehydration in the presence of proton (H<sup>+</sup>):

(1). Protonation of the alcohol:



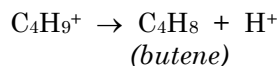
(2). Elimination of water:



\* Corresponding Author.

Email: melia@itb.ac.id (M. L. Gunawan)

(3). Formation of butene:



The reaction pathways for 1-butanol (n-butanol) dehydration to butenes and dibutyl ether are described in Figure 1.

The dehydration of butanol occurs in controlled conditions to maximize butene output and reduce by-products [4]. Temperature, pressure, and the concentration of the acid catalyst are critical determinants of the reaction's efficiency and selectivity [5]. The reaction is generally conducted at elevated temperatures between 150 °C and 250 °C to facilitate the dehydration at an efficient rate [6]. Higher temperatures facilitate the elimination reaction by supplying the requisite activation energy for the generation of the carbocation intermediate and the subsequent elimination of water [7,8].

The industrial application of butanol dehydration is crucial in the generation of butene, which acts as a fundamental precursor in the synthesis of diverse chemicals and polymers [9]. Butene is utilized in the synthesis of polyethylene and other polymers, in addition to the production of significant chemical intermediates like butadiene. Additionally, butene is used as a feedstock in the production of fuel additives and many specialty chemicals [10].

Zeolites are a category of microporous aluminosilicate minerals extensively employed as catalysts in diverse chemical processes, due to their unique structural characteristics, including large surface area, thermal stability, and molecular sieve capability [11]. The two-dimensional structure of zeolite (aluminosilicate) is shown in Figure 2. La-Y zeolite, a variant of commercial Y-type zeolite, has garnered considerable interest for its efficacy in catalytic

processes, especially in the dehydration of alcohols such as n-butanol to yield olefins like butene [12]. (Note: Lanthanum (La) is classified as a rare earth element).

La-Y zeolite is a modified variant of Y-zeolite, distinguished by its faujasite structure, which features a three-dimensional network of aluminosilicate tetrahedra. The addition of lanthanum (La) ions into the framework improves the catalytic characteristics of the zeolite [14]. Lanthanum ions stabilize the zeolite structure and enhance the catalyst's acidity by generating more potential acid sites [15]. The augmented acidic sites are essential for facilitating the dehydration of alcohols, as they proficiently donate protons to promote the elimination of water molecules from alcohol substrates [16]. The dehydration of n-butanol using La-Y zeolite involves multiple stages. n-Butanol first adsorbs onto the acid sites of the zeolite surface. The strong Brønsted acid sites provided by the La-Y zeolite promote the protonation of the hydroxyl group in n-butanol, resulting in the formation of a carbocation intermediate. This intermediate is very reactive and, in an acidic environment,

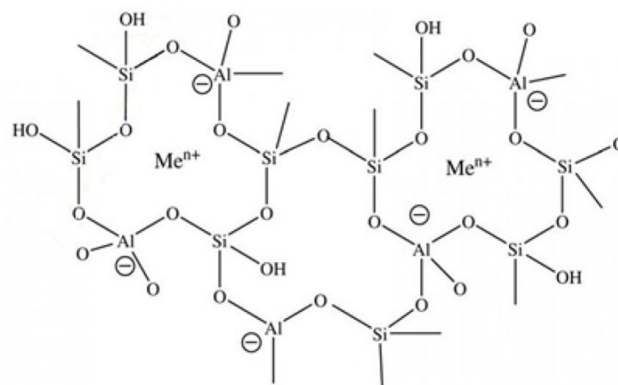


Figure 2. Zeolite structure [11].

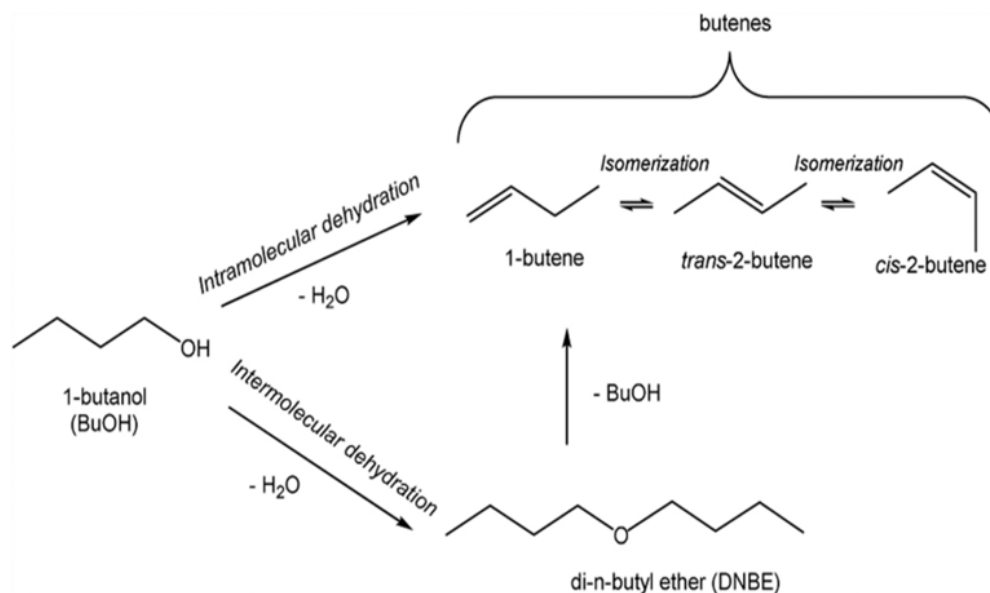


Figure 1. The reaction pathways for 1-butanol dehydration [3].

undergoes dehydration to create a butene molecule. The reaction predominantly produces 1-butene; however, isomerization may transpire under specific conditions, resulting in the formation of 2-butene. The function of La-Y zeolite in this process is dual function. It offers an extensive surface area for the adsorption and activation of n-butanol molecules and presents robust acid sites to promote protonation and subsequent dehydration processes. The microporous characteristics of the zeolite guarantee that the reaction transpires in a restricted environment, hence improving selectivity for preferred products such as butene.

Numerous parameters affect the efficiency and selectivity of n-butanol dehydration on La-Y zeolite, such as temperature, space velocity, and the presence of co-reactants or contaminants. The dehydration reaction is endothermic, indicating that it necessitates heat to occur. High temperatures often enhance the pace of n-butanol dehydration by supplying the requisite energy to surmount the activation barrier of the process. Excessively high temperatures can induce side reactions, including cracking and polymerization, which diminish selectivity for butene [17,18]. The duration of interaction between the reactants and the catalyst, commonly known as space velocity, is also crucial. Reduced space velocities (prolonged contact durations) often improve the conversion of n-butanol, although they may also raise the risk of adverse reactions. In contrast, increasing space velocities diminish contact time, perhaps restricting conversion while enhancing selectivity for butene.

Over time, the active sites of La-Y zeolite may become deactivated due to coke formation, wherein carbonaceous residues accumulate on the catalyst surface, obstructing active sites. The catalyst must be regenerated by combusting the coke at higher temperatures to restore its activity [3,18,19]. The formation of coke deposits frequently accompanies the reactions of petrochemical compounds, especially when the employed solid catalyst might facilitate cracking processes. This pertains to commercial cracking catalysts, which are prevalent catalysts utilized in the cracking processes of petroleum refineries. The coke produced may be strongly adsorbed onto the catalyst's active sites or obstruct the catalytic pores, hence reducing the active surface area [21]. The impact of coke formation on the reaction rate is typically represented by empirical correlations, suggesting that establishing a mechanistic or phenomenological kinetic equation for coke production is challenging. This occurs because coke is produced concurrently with other reaction products, either via parallel or sequential methods.

In the dehydration of n-butanol over zeolite-based catalysts, water is produced as a co-product

alongside olefins and influences coke formation and catalyst stability. Water can inhibit coke deposition by competitively adsorbing on Brønsted acid sites and reducing the effective acid strength, thereby suppressing secondary reactions such as oligomerization, cyclization, and aromatization that lead to coke precursors. In addition, steam may contribute to partial coke removal through gasification reactions [17,19,22,23]. As a result, coke formation during alcohol dehydration is generally less severe than in hydrocarbon cracking or olefin conversion processes. However, prolonged exposure to steam at elevated temperatures can induce dealumination of the zeolite framework, altering acid site distribution and accelerating catalyst deactivation [19,22-24]. Because coke deposition is strongly governed by temperature, time on stream, and residence time, its quantitative evaluation is essential for developing reliable deactivation models. Such models enable accurate prediction of catalyst deactivation, optimization of regeneration strategies, and improved process stability and olefin selectivity during n-butanol dehydration over zeolite-Y catalysts.

The relationship between reaction conditions and catalyst properties with coke formation and reaction rate is generally expressed in the form of empirical equations. This indicates that the kinetic equation for coke formation is not easy to develop or formulate. Voorhies (Froment & Bischoff and Aguayo) formulated the following empirical relation of coke formation with reaction time during the gas oil catalytic cracking [20,21]:

$$C_C = bt^m \quad (1)$$

in which:  $0.5 < m < 1$ ,  $t$  = reaction time,  $C_C$  = coke concentration, and  $b$  is an empirical coke deposition constant, and  $m$  is the time exponent reflecting the rate and mechanism of coke formation. Equation (1) is henceforth referred to as Model-1. The Voorhies model does not explicitly resolve individual elementary steps of coke formation; instead, it lumps the combined effects of secondary reactions, oligomerization, and condensation processes leading to carbonaceous deposits on the catalyst surface. At different temperatures, the constant  $b$  may have different values. According to the Arrhenius law, the reaction rate constant varies exponentially with temperature ( $T$ ), where  $E_a$  is the activation energy,  $R$  is the gas constant, and  $k_0$  is the Arrhenius constant.

$$k = k_0 \exp\left(\frac{-E_a}{RT}\right) \quad (1a)$$

Coke formation occurs concurrently with other reaction products through complex parallel and consecutive pathways. Consequently, the

coke formation rate is influenced by the reaction network, operating conditions (e.g., temperature), and catalyst activity, which progressively declines due to coke deposition on the catalyst surface. Therefore, a comprehensive kinetic model must be formulated by simultaneously solving the coke formation kinetics and the catalyst deactivation model in order to accurately describe the evolution of catalytic activity and overall reaction performance.

In 1976, Dumez and Froment proposed an equation for the rate of coke formation as a function of catalyst activity, i.e. [21]:

$$\frac{dC_C}{dt} = r_C^0 \phi_C \quad (2)$$

in which:  $r_C^0$  is the initial coking rate and  $\phi_C$  is catalyst activity during the coking process.

Dumez and Froment also proposed five models relating catalyst activity ( $\phi_C$ ) to coke deposit concentration ( $C_C$ ). These are [21]:

$$\phi_C = \exp(-\alpha C_C) \quad (3a)$$

$$\phi_C = 1 - \alpha C_C \quad (3b)$$

$$\phi_C = (1 - \alpha C_C)^2 \quad (3c)$$

$$\phi_C = \frac{1}{1 + \alpha C_C} \quad (3d)$$

$$\phi_C = \frac{1}{(1 + \alpha C_C)^2} \quad (3e)$$

Insertion of each of these equations into the model of coking rate (Equation (2)) followed by integration gives, respectively [21]:

$$C_C = \frac{1}{\alpha} \ln(1 + \alpha r_C^0 t) \quad (4a)$$

$$C_C = \frac{1}{\alpha} [1 - \exp(-\alpha r_C^0 t)] \quad (4b)$$

$$C_C = \frac{1}{\alpha} \left[ 1 - \frac{1}{1 + \alpha r_C^0 t} \right] \quad (4c)$$

$$C_C = \frac{1}{\alpha} [\sqrt{2\alpha r_C^0 t + 1} - 1] \quad (4d)$$

$$C_C = \frac{1}{\alpha} [\sqrt[3]{3\alpha r_C^0 t + 1} - 1] \quad (4e)$$

From this point forward, Equations (4a) to (4e) are designated as Model-4a), Model-4b), and so forth. The parameters  $\alpha$  and  $r_C^0$  are derived from the regression of experimental coking data utilizing the least squares method. According to Dumez and Froment, Model-4a) is generally the most compatible equation. However, Dumez and Froment did not further elucidate the relationship between the model parameters and either reaction temperature, space time or time on stream (TOS) of the catalyst.

Despite extensive studies on alcohol dehydration over zeolitic catalyst, quantitative assessment of coke deposition models for *n*-butanol dehydration conditions on commercial cracking catalyst matrices remains limited. To address this gap, the present study systematically compares the performance of two representative coke-deposition / deactivation models (Model-1

and Model-4, based on reference [21]) against experimental coke data. Key kinetic and deactivation parameters are estimated through rigorous fitting procedures, together with their corresponding confidence metrics, and the resulting model trends are interpreted in light of catalyst characterization results. Overall, this study assesses the applicability of both models by identifying their optimal fits and parameter values for the coke deposition process during *n*-butanol dehydration over a commercial zeolite-Y-based cracking catalyst, thereby providing a practical framework for predicting catalyst deactivation behavior, supports catalyst selection/regeneration strategy, and improves process reliability/selectivity.

## 2. Materials and Methods

The dehydration of *n*-butanol was carried out in an isothermal fixed-bed reactor setup illustrated in Figure 3. *n*-Butanol was infused into the reactor at a rate of 0.0428 g/minute via a syringe pump. The carrier gas (N<sub>2</sub>) flow rate was sustained at 10 mL/minute, as measured at ambient temperature and pressure. The reaction temperature varied between 400 °C and 475 °C. The weight of the commercial cracking catalyst forming the fixed bed varied from 0.1 g to 3 g. A fresh catalyst sample was used for each experimental run. The experiments were conducted in a continuous-flow reactor, and for each run, observations were carried out over a catalyst's time-on-stream (TOS) ranging from 15 to 390 minutes.

The coke content on the spent catalyst was determined gravimetrically for each experimental run. The spent catalyst was first dried in an oven at 110 °C until a constant weight was achieved, which was often after 4 hours, to remove water and unreacted butanol. Subsequently, it was calcined in a furnace at a temperature of 500 °C for 24 hours to entirely burn the deposited coke [24]. The amount of coke deposited was determined by the difference in catalyst weight prior to and after the calcination process. The coke content ( $C_C$ ) is expressed as the mass of coke per mass of fresh catalyst basis (g.coke/g.coke-free catalyst).

$$C_C = \frac{(m_0 - m_2) - (m_0 - m_1)}{m_2} = \frac{(m_1 - m_2)}{m_2} \quad (5)$$

in which,  $m_0$  is mass of the spent catalyst sample (g),  $m_1$  is mass of the catalyst sample after drying in an oven for 4 hours at 110 °C (g),  $m_2$  is mass of the catalyst sample after calcination in a furnace for 24 hours at 500 °C (g).

In continuous reactor systems, the space time is defined as the ratio of reactor volume to the volumetric flow rate of the feed stream. For heterogeneous catalytic reactions involving solid

catalysts, space time is more appropriately expressed in terms of catalyst loading. Accordingly, space time is defined as the ratio of catalyst mass to the molar flow rate of the reactant. Mathematically, space time is expressed as:

$$\tau = \frac{W}{F_{A0}} \quad (6)$$

where  $\tau$  is the space time (g. catalyst h.mol<sup>-1</sup>),  $W$  is the mass of catalyst in the reactor (g), and  $F_{A0}$  is the inlet molar flow rate of *n*-butanol (mol.h<sup>-1</sup>). This definition is particularly appropriate for packed-bed catalytic reactors, where the reaction rate and catalyst deactivation are directly related to the catalyst mass and reactant molar throughput.

The properties of catalyst used in this study was characterized using some analysis instruments. The silica/alumina ratio (Si/Al) was analysed by Rigaku NEX CG X-ray Fluorescence (XRF) serial CG1544 instrument with helium atmosphere. The crystallinity of catalyst analysed using Bruker D8 Advance X-ray Diffractometer (XRD) with radiation of Cu-K $\alpha$  in the range of 2 $\theta$  of 5–60°. The specific surface area, average pore diameter, average pore volume, and adsorption/desorption data for Langmuir isotherm were analysed by Nitrogen-

physisorption method using a Micromeritics® Tristar II Plus 3.01 instrument. The surface morphology of catalyst was captured using the Hitachi scanning electron microscope (SEM) SU3500 instrument with 10 kV of accelerated voltage.

Model equations (Model-1 and Model-4) were used to describe coke accumulation and its effect on catalyst deactivation. Model parameters were estimated by fitting experimental coke content data using a nonlinear least-squares method, minimizing the objective function defined as:

$$SS(\theta) = \sum_{i=1}^N (C_{C,i}^{data} - C_{C,i}^{model}(\theta))^2 \quad (7)$$

where:  $SS(\theta)$  is the objective function,  $C_{C,i}^{data}$  and  $C_{C,i}^{model}$  are the experimental data and predicted coke content at data point  $i$ , respectively,  $\theta$  donates the model parameters, and  $N$  is the total number of experimental data points. Parameter estimation and regression analysis were performed using MATLAB software (version R2022a, MathWorks Inc.). Model performance was evaluated using the coefficient of determination ( $R^2$ ). The estimated parameters were also assessed for consistency with the proposed coke formation and catalyst deactivation mechanisms on acidic zeolite sites.

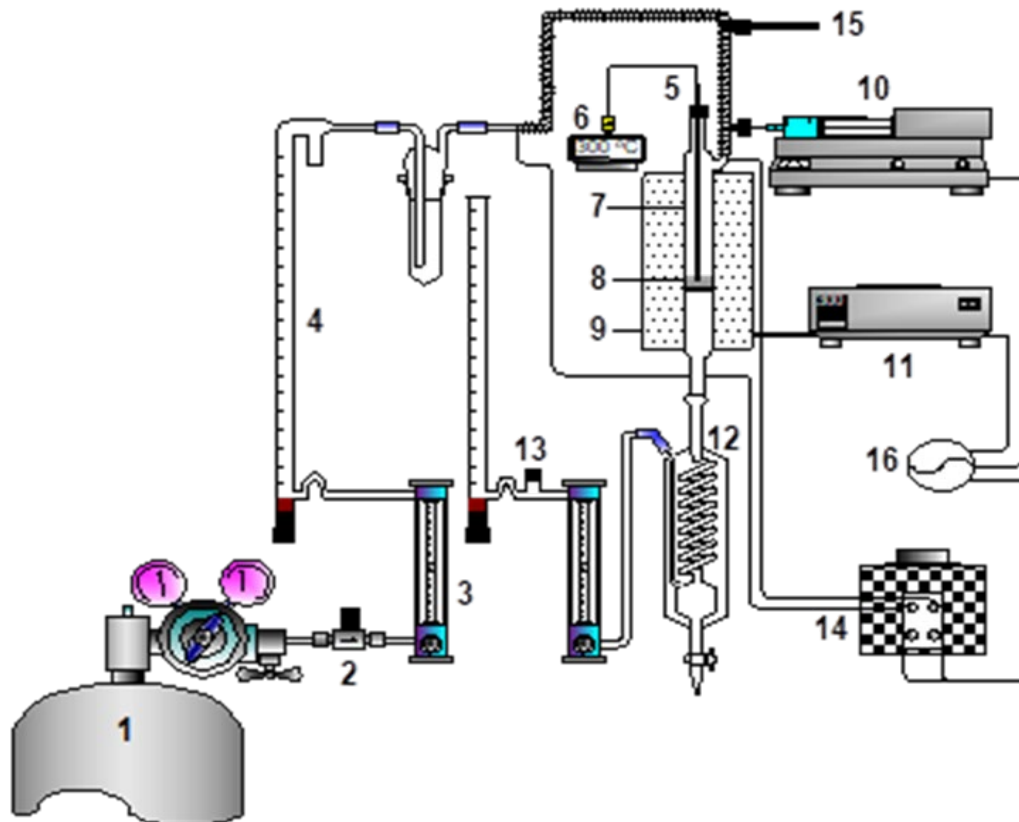


Figure 3. The experimental set-up. 1= Nitrogen (N<sub>2</sub>) gas cylinder, 2= Mass flow controller, 3= Rotameter 4 = Soap bubble flowmeter, 5 = Thermocouple, 6 = Thermometer display, 7 = Reactor, 8 = Catalyst bed, 9.= Furnace, 10 = Syringe pump, 11 = Temperature controller, 12 = Condenser, 13 = Gas sample port, 14 = Variac, 15 = Thermometer, 16 = AC electric current source

### 3. Results and Discussion

#### 3.1. Characterization of La-Y Zeolite Catalyst

The commercial zeolite-Y catalyst utilized in this study was thoroughly characterized through several analytical techniques to evaluate its structural, textural, and chemical properties, which are crucial in understanding its catalytic performance, particularly in the dehydration of n-butanol to butenes. Nitrogen physisorption analysis was used to assess the textural properties of the catalyst, revealing that the average pore diameter of the zeolite was 57.208 Å. This value confirms the presence of relatively large mesopores, aligning with the observed pore volume of 0.602 cm<sup>3</sup>/g. Mesoporous materials, by definition, have pore sizes ranging between 20 to 500 Å, which enhances the diffusion of molecules into the catalyst, thereby improving its effectiveness in gas-phase reactions like n-butanol dehydration. Furthermore, the surface area of 350–390 m<sup>2</sup>/g provides a substantial number of active sites for the reaction, contributing to the catalyst's overall efficiency. The bulk density and skeletal density of the catalyst are 0.5568 g/cm<sup>3</sup> and 1.2727 g/cm<sup>3</sup>, respectively. The catalyst porosity is 56.25%. The adsorption isotherm obtained from the physisorption analysis is identified as Type IV isotherms with a distinct hysteresis loop, which is characteristic of mesoporous materials. The shape of the isotherm curve generally indicates the presence of capillary condensation in mesopores, further corroborating the mesoporous nature of the catalyst (see Figure 4a).

In addition to physisorption analysis, the zeolite-Y catalyst was characterized by X-ray fluorescence (XRF) to determine its chemical composition. The results showed a Si/Al ratio of 6, indicating moderate acidity of the catalyst [19]. The silica-to-alumina ratio in the zeolite framework plays a key role in determining its acidic properties, which are critical for alcohol

dehydration reactions.. The moderate acidity of the zeolite-Y catalyst makes it ideal for this reaction and butene skeletal isomerization as overly acidic catalysts can promote unwanted side reactions, such as cracking, leading to the formation of undesired products like coke [19]. A pronounced difference in adsorption capacity is observed between the fresh and spent zeolite-Y over the entire pressure range. The fresh zeolite-Y catalyst exhibits a significantly higher N<sub>2</sub> uptake, reaching approximately 390–400 cm<sup>3</sup>.g<sup>-1</sup> (STP) at  $P/P_0 \rightarrow 1$ , whereas the spent zeolite-Y catalyst shows a reduced capacity of approximately 340–350 cm<sup>3</sup>.g<sup>-1</sup> (STP). This reduction clearly indicates a loss of accessible surface area and pore volume after practical operation, which is primarily attributed to partial pore blocking and surface coverage by coke-containing species formed during the n-butanol dehydration reaction. The hysteresis loop of the spent catalyst is noticeably narrower and slightly shifted compared to that of the fresh catalyst. This phenomenon indicates structural modification of the pore network, including narrowing of pore entrances and partial collapse of smaller mesopores caused by coke deposition. The observed narrowing of the hysteresis loop further supports this interpretation, confirming the presence of diffusion limitations imposed by coke precursors.

Figure 4b show that the pore size distribution of the fresh and spent catalysts shows a similar overall profile, with a dominant mesopore peak centered at approximately 50–60 Å, indicating that the mesoporous structure of the catalyst is largely preserved after reaction. However, the fresh catalyst exhibits a slightly higher pore volume at the main mesopore peak compared to the spent catalyst. The reduced mesopore volume observed for the spent catalyst suggests partial pore blockage, most likely due to the deposition of carbonaceous species formed during the reaction. This blockage decreases pore accessibility without

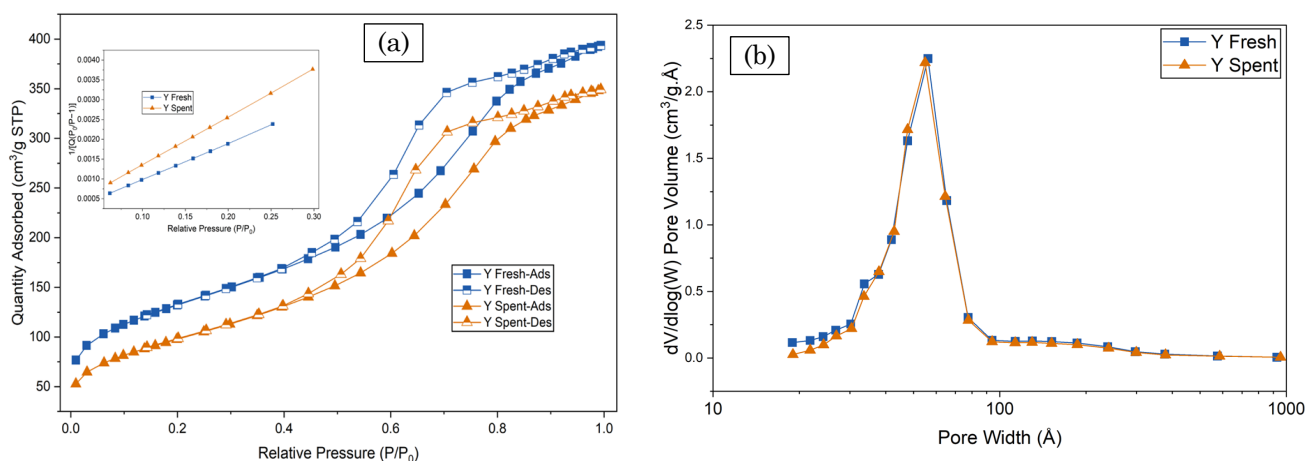


Figure 4. Isotherm Langmuir for fresh and one of spent zeolite-Y catalyst (a) and pore distribution of fresh and one of spent zeolite-catalyst (b)

causing significant structural collapse. At larger pore widths (>100 Å), both catalysts display nearly identical distributions, indicating that macroporosity remains unaffected by catalyst usage. These results imply that catalyst deactivation is mainly associated with mesopore obstruction rather than irreversible framework degradation, suggesting that catalyst regeneration may restore pore accessibility and performance.

The X-ray diffraction (XRD) pattern, shown in Figure 5(a), provides insight into the crystallinity and phase purity of the zeolite-Y catalyst. The diffraction peaks observed at 2-theta angles, particularly around 20°, are consistent with the characteristic diffraction pattern of zeolite Y, confirming the retention of its crystalline structure after synthesis or potential modification processes. The broadness of the peaks may suggest some degree of amorphization or partial disorder in the crystal lattice, but overall, the material retains its zeolitic structure. Crystallinity is a key factor in maintaining the integrity of the porous framework, which is necessary for the catalyst's longevity and stability under reaction conditions.

Figure 5(b) displays a scanning electron microscopy (SEM) image of the zeolite-Y catalyst, providing a visual representation of its surface morphology. The image reveals that the catalyst consists of spherical particles with rough surfaces, which is typical for zeolites. These spheres appear to be composed of smaller crystallites aggregated together. The rough surface texture enhances the surface area available for catalysis, allowing better interaction between the reactant molecules and the active sites. The particle size distribution is relatively uniform, with an average size in the micrometer range, which is advantageous for maintaining good flow characteristics in a fixed-bed reactor system. Additionally, the spherical morphology observed in the SEM image indicates good mechanical strength, which is essential for industrial applications, as it minimizes catalyst

attrition during use. Taken together, the characterization results of the zeolite-Y catalyst confirm that it possesses the necessary physical and chemical properties for efficient catalysis in the dehydration of n-butanol to butenes. The moderate acidity, mesoporous structure, and high surface area ensure that the catalyst can effectively facilitate the desired reaction while minimizing the formation of undesirable by-products such as coke [19].

Additionally, crystallinity and mechanical stability, as indicated by the XRD and SEM analyses, ensure the catalyst's robustness under the operating conditions, making it suitable for prolonged use in industrial settings. The next phase of this study focuses on kinetic modeling of coke formation, as the accumulation of coke on the catalyst surface can significantly hinder its performance over time.

### 3.2. Coke Content vs. Time on Stream (TOS)

The underlying assumption of the Voorhies model is that coke formation proceeds under approximately steady reaction conditions, where the overall rate of coke accumulation can be correlated with time-on-stream through an empirical power-law relationship. The exponent  $m$  provides insight into the dominant coke formation behavior: values of  $m$  close to unity indicate approximately linear accumulation of coke, whereas higher values suggest accelerating coke deposition due to pore blockage, increased residence time of heavy intermediates, or autocatalytic coke growth. In the context of n-butanol dehydration over acidic zeolite-Y-based catalysts, this model represents the net outcome of dehydration, oligomerization, and cracking reactions that contribute to coke precursor formation. The measured coke content of the spent catalysts from n-butanol dehydration at various temperatures and time on stream (TOS) was presented in Table 1. The longer the catalyst was utilized, the higher the coke content. The best-fit

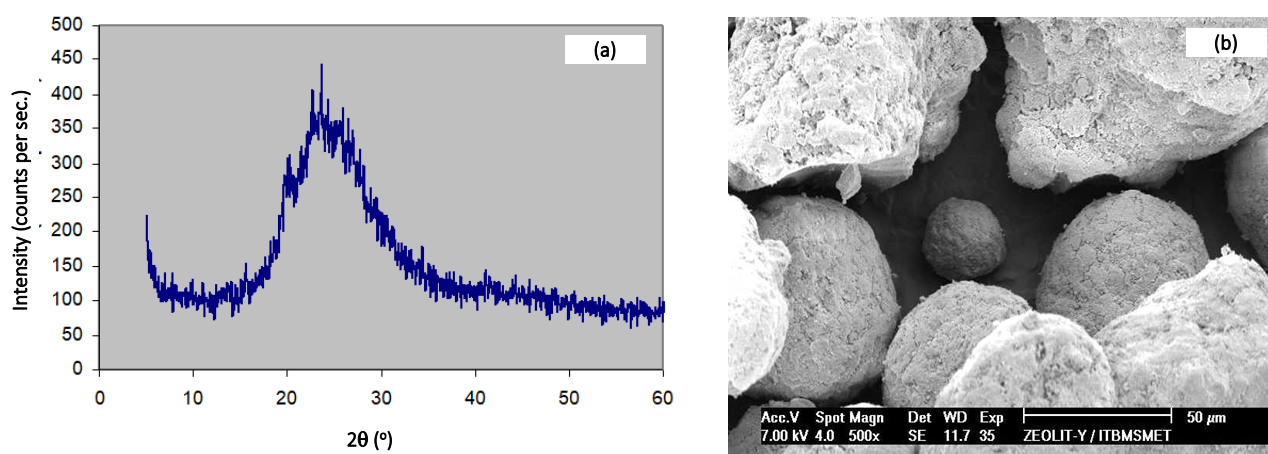


Figure 5. (a) The X-Ray Diffractogram pattern of zeolite commercial, (b) The Scanning Electron Microscope (SEM) image of zeolite commercial.

parameter values of the various models examined are shown in Table 2.

The quality of the fit is represented by the correlation coefficient,  $R^2$ ; a perfect fit gives the value of the correlation coefficient  $R^2$  equal to 1 (one). Therefore, based on the statistical significance ( $R^2$ ) of the obtained parameter values, the best-fit models for coke deposition on the catalyst of the present work are Model-1 and Model-4a. This agrees with the finding of Dumez and Froment that Model-4a is generally better than the other phenomenological models. Figure 2 shows the quality of the fit obtained. In a fixed or constant space-time, varying durations of catalyst usage (time on stream, TOS) indicate that the catalyst processes the same n-butanol feed flow but during different operational periods.

Table 2 indicates that the values of  $b$  and  $m$  in Model-1, as well as  $\alpha$  and  $rc^0$  in Model-4a,

appear to be dependent on temperature ( $T$ ). Subsequent analysis indicates that at a reaction temperature ( $T$ ) ranging from 673 K to 748 K (400 to 475 °C), the most effective equations correlating the concentration of coke deposits ( $C_c$ , in g coke/g clean-catalyst or g coke/g coke-free zeolite) with time on stream ( $t$ , in hours) are as follows:

(1). Based on Model-1:

$$C_c = 0.254 \exp(-1157.3/T) t^{0.00187T-1.0218} \quad (8)$$

The correlation coefficient ( $R^2$ ) for the parameter of  $b$  is 0.979, and that for the parameter of  $m$  is 0.998. A three-dimensional profile curve for this model is presented in Figure 7a.

2. Based on Model-4a:

$$C_c = \frac{1}{0.0197 \exp(5787.2/T)} \ln(1 + 3.31 \times 10^{-9} t \exp(16436/T)) \quad (9)$$

Table 1. Deposit of coke on a commercial cracking catalyst used to catalyze dehydration of n-butanol at various reaction temperatures and time on stream (catalyst weight = 1 g, space time = 28.82 g-cat.h/mole n-butanol).

Time on stream (TOS), (minute)	$C_c$ (g.coke / g.coke-free catalyst) $\times 10^2$ at		
	400 °C	450 °C	475 °C
15	3.52	0.50	3.51
30	3.95	3.91	3.89
60	4.32	4.98	5.75
120	5.56	6.54	7.44
390	6.57	8.45	9.79

Table 2. Best-fit parameter values of Models 1 and 4a to 4e in describing the coke content of a commercial zeolite-Y catalyst as a function of time on stream ( $t$ ).

Model	Temp. (°C)	Parameters			$R^2$	
		$b \times 10^2$	$m \times 10^2$	$\alpha$		$rc^0$
1)	400	4.57	20.02		0.97	
	450	5.05	28.63		0.98	
	475	5.46	33.74		0.97	
4a)	400			104.92	$125.82 \times 10^{-2}$	0.97
	450			62.96	$40.89 \times 10^{-2}$	0.98
	475			43.24	$25.97 \times 10^{-2}$	0.98
4b)	400			20.23	$20.24 \times 10^{-2}$	0.44
	450			16.32	$14.68 \times 10^{-2}$	0.58
	475			13.54	$13.05 \times 10^{-2}$	0.74
4c)	400			17.73	$30.88 \times 10^{-2}$	0.74
	450			13.74	$20.59 \times 10^{-2}$	0.80
	485			10.89	$16.86 \times 10^{-2}$	0.91
4d)	400			$6.93 \times 10^{16}$	$1.09 \times 10^{-14}$	-
	450			$7.09 \times 10^{16}$	$8.90 \times 10^{-13}$	0.38
	475			$5.75 \times 10^{16}$	$5.70 \times 10^{-13}$	0.72

Note: coke content, in g/g coke-free catalyst; Reaction time (= time on stream / TOS) in hours  
Model-4e failed to give even a reasonable fit to the data.

The  $R^2$  value for parameter  $\alpha$  is 0.984, and that for parameter  $\tau c^0$  is 0.999. When both parameters are lumped, however, the value of  $R^2$  becomes 0.999. A three-dimensional profile curve for this model is shown in Figure 7b.

### 3.3. Coke Content vs Space Time

The other important process variable of a continuous heterogeneous catalytic tubular reactor is space time, i.e., catalyst weight divided by the feed flow rate. This variable represents the time required by the catalyst to process the amount of reactant in the reactor. Table 3 presents data on the coke content of spent commercial cracking catalysts employed to dehydrate n-butanol for 390 minutes (TOS) at various space times. The results of curve fitting the models to the experimental data, based on the assumption that the relationship between the

concentration of deposited coke and space-time adheres to the models, are provided in Tables 4 and Figure 8. Table 4 displays the optimal parameter values for the various models analysed. The parameters of the model also denote the temperature function. The evaluation results for the temperature ( $T$ ) range of 673 K to 748 K, based on an empirical relationship between the concentration of coke deposit ( $C_C$ , in g coke/g coke-free catalyst) and space time ( $\tau$ , in hours), are as follows:

(1). Based on Model-1:  

$$C_C = 0.2664 \exp(-1064.3/T) \tau^{0.00087-0.504} \quad (10)$$

The correlation coefficient ( $R^2$ ) for parameter  $b$  is 0.99, and that for parameter  $m$  is 0.99. A three-dimensional profile curve for this model is presented in Figure 9a.

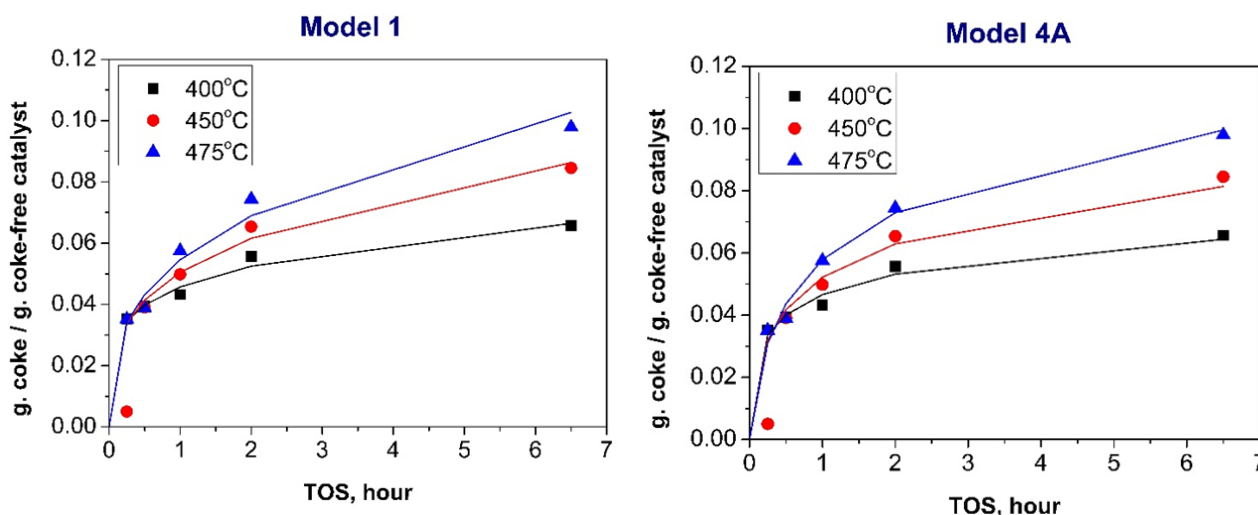


Figure 6. Best fits of (a) Model-1) and (b) Model-4 a) to the experimental data on coke content of a commercial cracking catalyst used to dehydrate n-butanol (space time = 28.82 g cat.h/mole n-butanol, weight of catalyst bed = 1 g).

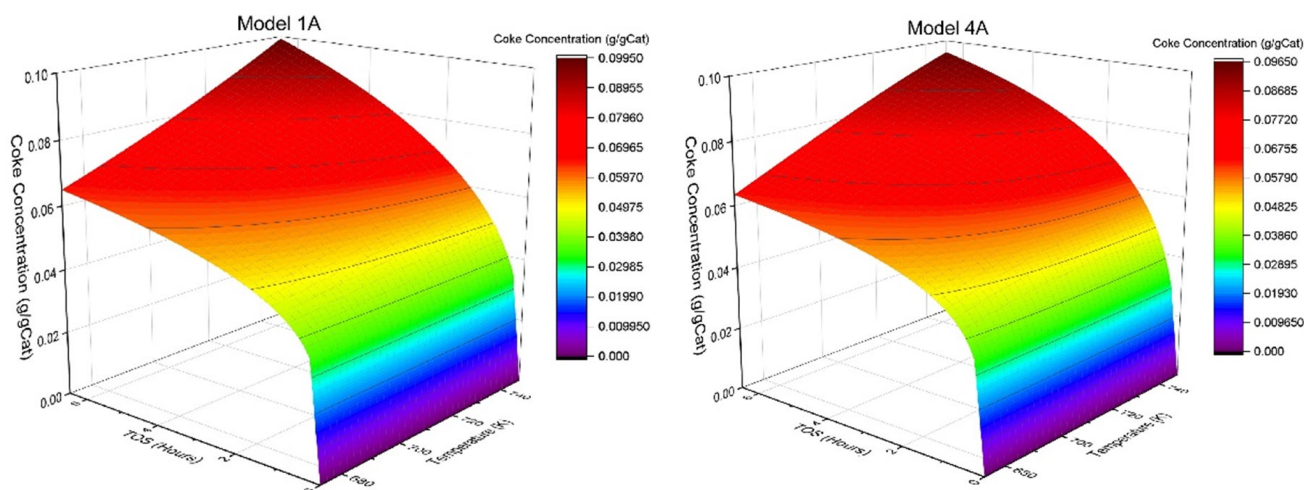


Figure 7. Three-dimensional profile curves of (a) extended Model-1), i.e. Equation (8), and (b) extended Model-4a), namely Equation (9), representing the coke content as functions of temperature ( $T$ ) and time on stream ( $t$ ).

(2). Based on Model-4a:

$$C_c = \frac{1}{0.32 \times 10^{-2} \exp(7600/T)} \ln(1 + 1.35 \times 10^{-36} \tau \exp(65.1 \times 10^3/T)) \quad (11)$$

The R<sup>2</sup> value for parameter  $\alpha$  is 0.99, and that for parameter  $r_c^0$  is 0.96. When both parameters are lumped, however, the value of R<sup>2</sup> becomes 0.97. A three-dimensional profile curve for this model is shown in Figure 9 b.

### 3.4. Interpretation of Fitted Parameters and Comparison of Coke Deposition Models

For Model-1 proposed by Voorhies, the fitted parameters  $b$  and  $m$  characterize the empirical coke deposition behavior during n-butanol dehydration. The parameter  $b$  reflects the initial tendency of coke formation on the fresh catalyst

Table 3. Deposit of coke on a commercial zeolite-Y used to catalyze dehydration of n-butanol at various reaction temperatures and space-time (at time on stream (TOS) of 390 minutes).

Cat. weight, g	Space Time g cat.h/mole	C <sub>c</sub> (g.coke / g.coke-free catalyst) × 10 <sup>2</sup> at		
		400 °C	450 °C	475 °C
0.1	2.882	5.77	6.74	7.69
0.2	5.763	6.22	7.49	7.55
0.5	14.408	6.56	7.94	8.73
1	28.816	6.57	8.45	9.79
1.5	43.224	6.92	9.53	10.60
2	57.632	6.84	8.96	10.72
2.5	72.04	7.03	9.67	10.99
3	86.449	7.44	9.76	10.79

Table 4. Best-fit parameter values of Models 1 and 4a to 4e in describing the coke content of a commercial zeolite-Y catalyst as a function of space time ( $\tau$ ).

Model	Temp. (°C)	$b \times 10^2$	$m \times 10^2$	$\alpha$	$r_c^0$	R <sup>2</sup>
1)	400	5.49	6.05			0.92
	450	6.07	10.66			0.95
	475	6.34	12.76			0.95
4 a)	400			267.3	8275.3	0.98
	450			111.04	5.4	0.94
	475			69.86	0.5	0.95
4 b)	400			15.11	4.52 × 10 <sup>-2</sup>	0.42
	450			11.71	4.19 × 10 <sup>-2</sup>	0.46
	475			9.34	1.19 × 10 <sup>-2</sup>	0.34
4 c)	400			14.62	12.47 × 10 <sup>-2</sup>	0.71
	450			11.02	8.12 × 10 <sup>-2</sup>	0.77
	475			8.54	2.31 × 10 <sup>-2</sup>	0.37

Note: coke content, in g/g coke-free catalysts ; Space-time =  $\tau$ , in hours.  
Model-4 d) and 4e) failed to give even a reasonable fit to the data.

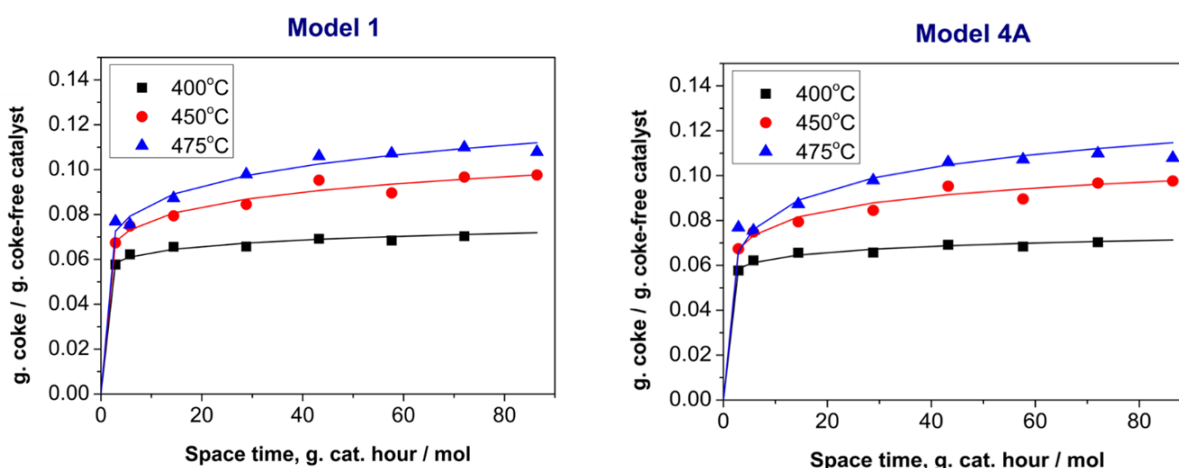


Figure 8. Best fits of (a) Model-1) and (b) Model-4 a) to the experimental data on coke content of a commercial cracking catalyst used to dehydrate n-butanol (at TOS = 390 minutes).

surface, while the exponent  $m$  describes the temporal evolution of coke accumulation. The obtained value of  $m$  indicates that coke formation does not increase linearly with time, suggesting the contribution of secondary reactions and progressive pore blockage on the zeolite-Y composite catalyst. This behavior is consistent with the known deactivation characteristics of acidic cracking catalysts reported in the literature.

For Model-4 proposed by Dumez–Froment, the fitted parameters  $a$  and  $r_c^0$  represent the initial coke formation tendency and the inhibitory effect of accumulated coke on further coke growth. The analytical forms derived from this model (Equations (4a–4e)) were evaluated by fitting experimental coke deposition data. Among these expressions, only Model-4a provided consistently high coefficients of determination ( $R^2 = 0.97–0.99$ ), comparable to those obtained with Model-1, while Models 4b–4e showed poor or physically unrealistic fitting behavior. The superior performance of Model-4a indicates that coke deposition follows a non-linear trend and is progressively inhibited by coke accumulation, likely due to pore blockage and reduced accessibility of acidic active sites. This inhibitory effect becomes more pronounced at longer time-on-stream, which cannot be fully captured by the simple power-law formulation of Model-1.

Overall, Model-1 provides an accurate empirical description of coke accumulation, while Model-4a offers a more physically realistic representation by incorporating the inhibitory effect of accumulated coke. Therefore, Model-1 and Model-4a are identified as the most appropriate models for describing coke formation and catalyst deactivation during *n*-butanol dehydration over zeolite-Y catalysts. A summary comparison of these models is presented in Table 5.

#### 4. Conclusion

This study provides a comparative assessment of empirical coke deposition models during *n*-butanol dehydration over a commercial zeolite-Y-based cracking catalyst, with emphasis on the kinetics and physical interpretation of catalyst deactivation. The main conclusions are as follows: (1). Coke formation occurs as a parallel and consecutive process during *n*-butanol dehydration, confirming that secondary cracking and condensation reactions on acidic zeolite sites contribute significantly to catalyst deactivation; (2). Coke accumulation is governed by temperature, space time ( $\tau$ ), and time-on-stream (TOS), demonstrating that coke deposition is controlled by both intrinsic reaction kinetics and transport limitations within the catalyst pore network; (3). The temporal evolution of coke deposition exhibits a decelerating trend, indicating progressive pore blockage and surface coverage, which reduces active site accessibility and inhibits further coke formation; (4). The Voorhies power-law model (Model-1) provides an accurate empirical description of coke accumulation, yielding excellent agreement with experimental data and confirming its suitability for representing overall coke deposition trends; (5). The Dumez–Froment-based empirical model (Model-4a), particularly its logarithmic form, provides a more mechanistically meaningful representation, as it explicitly captures the inhibitory effect of accumulated coke on subsequent coke formation. This behavior reflects the progressive loss of accessible active sites and increasing diffusion resistance within the catalyst structure; (6). The superior performance of the Dumez–Froment-based model demonstrates that coke deposition during *n*-butanol dehydration is inherently non-linear and self-inhibiting,

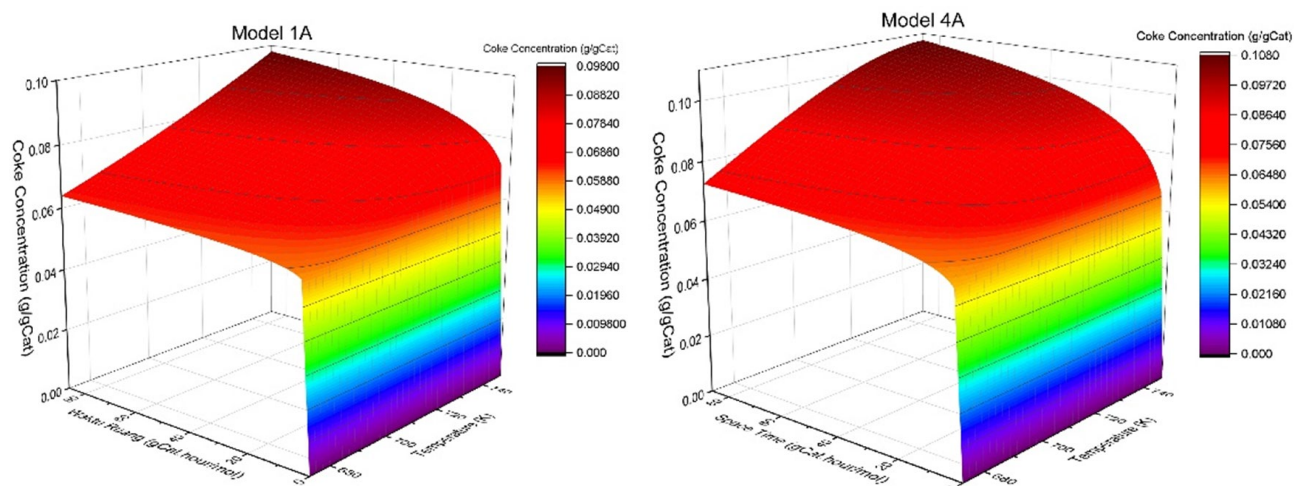


Figure 9. Three-dimensional profile curves of (a) extended Model-1), i.e. equation (10), and (b) extended Model-4a), namely Equation (11), representing the coke content as functions of temperature ( $T$ ) and space time ( $\tau$ )

highlighting the importance of incorporating deactivation effects into kinetic and reactor models; (7). The empirical models developed in this study provide a validated predictive framework for describing coke accumulation and catalyst deactivation, which is essential for reactor design, catalyst lifetime prediction, and process optimization in catalytic alcohol dehydration systems relevant to biofuel and olefin production; (8). This work contributes to improved understanding of coke-induced catalyst deactivation mechanisms on zeolite-based catalysts, providing experimentally validated models that bridge empirical observations and mechanistic interpretation of coke deposition dynamics.

### Acknowledgment

The authors gratefully acknowledge the supported and the financial support from P2MI-FTL, RU3P- 2024 and RK3P- 2025 Center for Catalysis and Reaction Engineering, Institut Teknologi Bandung- Indonesia.

### CRedit Author Statement

Author Contributions: Tri Partono Adhi: Visualization, Conceptualization, Writing-Reviewing and Editing. Melia Laniwati Gunawan: Conceptualization, Writing- Original draft preparation, Methodology, Reviewing and Editing. Subagjo: Methodology, Supervision. IGBN Makertihartha: Methodology, Supervision. Azizah Nabilah : Data curation, Visualization. Hanief Aulia: Data curation, Writing- Reviewing and Editing. All authors have read and agreed to the published version of the manuscript.

### References

- [1] de Reviere, A., Gunst, D., Sabbe, M.K., Reyniers, M.F., Verberckmoes, A. (2021). Dehydration of Butanol Towards Butenes over MFI, FAU and MOR: Influence of Zeolite Topology. *Catalysis Science & Technology*, 11(7), 2540-2559, DOI: 10.1039/D0CY02366C
- [2] de Reviere, A., Gilson, J.P., Valtchev, V., Thybaut, J.W., Sabbe, M.K., Verberckmoes, A. (2024). Enhancing the Catalytic Performance of H-ZSM-5 in Bio-butanol Dehydration on by Zeolite Crystal Engineering, *Applied Catalysis B: Environment and Energy*, 357, 124351, DOI: 10.1016/j.apcatb.2024.124351
- [3] Conesa, J.M., Morales, M.V., García-Bosch, N., Ramos, I.R., Guerrero-Ruiz, A. (2023). Graphite Supported Heteropoly Acid as a Regenerable Catalyst in the Dehydration of 1-Butanol to Butenes. *Catalysis Today*, 420, 114017. DOI: 10.1016/j.cattod.2023.01.024
- [4] Segovia-Hernández, J.G., Sánchez-Ramírez, E., Alcocer-García, H., Quiroz-Ramírez, J.J., Udagama, I.A., Mansouri, S.S. (2020). Analysis of Intensified Sustainable Schemes for Biobutanol Purification, *Chemical Engineering and Processing-Process Intensification*, 147, 107737, DOI: 10.1016/j.cep.2019.107737
- [5] de Reviere, A., Gunst, D., Sabbe, M., Verberckmoes, A. (2020). Sustainable Short-chain Olefin Production through Simultaneous Dehydration of Mixtures of 1-Butanol and Ethanol over HZSM-5 and  $\gamma$ -Al<sub>2</sub>O<sub>3</sub>, *Journal of Industrial and Engineering Chemistry*, 89, 257-272, DOI: 10.1016/j.jiec.2020.05.022
- [6] Kella, T., Vennathan, A.A., Dutta, S., Mal, S.S., Shee, D. (2021). Selective Dehydration of 1-Butanol to Butenes over Silica Supported Heteropoly Acid Catalysts: Mechanistic Aspect, *Molecular Catalysis*, 516, 111975, DOI: 10.1016/j.mcat.2021.111975
- [7] Chang, X. (2023). Understanding the Dehydration of Acetone, 1-Butanol, and Ethanol Fermentation-based Biofuel, *Energy Sources, Part A: Recovery, Utilization, and Environmental Effects*, 45(3), 8062-8075. DOI: 10.1080/15567036.2023.2225450

Table 5. Summary of comparison of Model-1 and Model-4.

Aspect	Model-1 : Voorhies	Model-4 : Dumez-Froment
Model nature	Empirical power-law	Empirical, rate-derived
Key assumption	Lumped coke growth	Coke inhibits its own formation
Parameters	$b = f$ (exponential of $T$ ) $m = f$ (linear to $T$ )	$\alpha = f$ (exponential of $1/T$ ) $rc^o = f$ (exponential of $1/T$ )
Coke growth behavior	Monotonic, power-law	Non-linear, saturating
Coke-activity relation	Implicit	Explicit
Physical interpretation	Limited	More meaningful
Prediction capability	Suitable for short-term trend	More accurate for full coke evolution
Model complexity	Simple	Moderate
Physical insight	Limited	Higher

- [8] Shi, Y., Weller, A.S., Blacker, A.J., Dyer, P.W. (2022). Conversion of Butanol to Propene in Flow: A Triple Dehydration, Isomerization and Metathesis Cascade. *Catalysis Communications*, 164, 106421, DOI: 10.1016/j.catcom.2022.106421
- [9] Chen, L., Lin, Z. (2021, December). Polyethylene: Properties, Production and Applications, In *2021 3rd International Academic Exchange Conference on Science and Technology Innovation (IAECST)* (pp. 1191-1196). IEEE, DOI: 10.1109/IAECST54258.2021.9695646
- [10] Díaz Velázquez, H., Likhanova, N., Aljammal, N., Verpoort, F., Martínez-Palou, R. (2020). New Insights into the Progress on the Isobutane/butene Alkylation Reaction and Related Processes for High-quality Fuel Production A Critical Review. *Energy & Fuels*, 34(12), 15525-15556. DOI: 10.1021/acs.energyfuels.0c02962
- [11] Fitriyah, F., Krisnandi, Y.K. (2023). Sintesis Zeolit dari Bahan Alam dan Limbah Buangan. *Jurnal Serambi Engineering*, 8(3), 6200-6207, DOI: 10.32672/jse.v8i3.6079
- [12] Vu, H.T., Goepel, M., Gläser, R. (2021). Improving the Hydrothermal Stability of Zeolite Y by La<sup>3+</sup> Cation Exchange as a Catalyst for the Aqueous-phase Hydrogenation of Levulinic Acid. *RSC Advances*, 11(10), 5568-5579, DOI: 10.1039/d0ra08907a
- [13] He, J., Lin, L., Liu, M., Miao, C., Wu, Z., Chen, R., ... & Luo, W. (2022). A durable Ni/La-Y Catalyst for Efficient Hydrogenation of  $\gamma$ -Valerolactone into Pentanoic Biofuels. *Journal of Energy Chemistry*, 70, 347-355, DOI: 10.1016/j.jechem.2022.02.011
- [14] He, J., Wu, Z., Gu, Q., Liu, Y., Chu, S., Chen, S., ... & Luo, W. (2021). Zeolite - Tailored Active Site Proximity for the Efficient Production of Pentanoic Biofuels. *Angewandte Chemie*, 133(44), 23906-23914, DOI: 10.1002/anie.202108170
- [15] Yu, S., Yan, J., Lin, W., Long, J., Liu, S.B. (2021). Effects of Lanthanum Incorporation on Stability, Acidity and Catalytic Performance of Y Zeolites. *Catalysis Letters*, 151, 698-712, DOI: 10.1007/s10562-020-03357-y
- [16] Potter, M.E., Amsler, J., Spiske, L., Plessow, P. N., Asare, T., Carravetta, M., ... & Armstrong, L.M. (2023). Combining Theoretical and Experimental Methods to Probe Confinement within Microporous Solid Acid Catalysts for Alcohol Dehydration. *ACS Catalysis*, 13(9), 5955-5968, DOI: 10.1021/acscatal.3c00352
- [17] Bartholomew, C.H. (2001) Mechanisms of Catalyst Deactivation, *Applied Catalysis A: General*, 212 (1-2), 17-60. DOI: 10.1016/S0926-860X(00)00843-7
- [18] Guisnet, M., Magnoux, P. (2001), Organic Chemistry of Coke Formation, *Applied Catalysis A: General*, 212 (1-2), 83-96. DOI: 10.1016/S0926-860X(00)00845-0
- [19] Kulprathipanja, S. (2010). *Zeolites in Industrial Separation and Catalysis*, Wiley-VCH Verlag GmbH & Co. KGaA, Weinheim, ISBN: 978-3-527-32505-4, 420-528
- [20] Bilbao, J., Aguayo, A.T., Arandes, J.M. (1985). Coke deposition on silica-alumina catalysts in dehydration reactions. *Industrial & Engineering Chemistry Product Research and Development*, 24(4), 531-539, DOI: 10.1021/I300020A009
- [21] Froment, G.F., Bischoff, K.B., Wilde, J. De. (2010). *Chemical Reactor Analysis and Design*. 3rd Edition, Wiley, ISBN: 978-0-470-56541-4.
- [22] Guisnet, M., Andy, P., Gnep, N.S., Travers, C., Benazzi, E. (1998). Comments on "Skeletal Isomerization of Butene: On the Role of the Bimolecular Mechanism". *Ind. Eng. Chem. Res.* 37, 300–302, DOI: 10.1021/ie970829v
- [23] Aguayo, A.T., Gayubo, A.G., Atutxa, A., Olazar, M., Bilbao, J. (2002) Catalyst Deactivation by Coke in the Transformation of Aqueous Ethanol into Hydrocarbons, Kinetic Modeling and Acidity Deterioration of the Catalyst, *Ind. Eng. Chem. Res.*, 41, 4216-4224. DOI: 10.1021/ie020068i
- [24] Diaz, M., Epelde, E., Valecillos, J., Izaddoust, S., Aguayo, A.T., Bilbao, J. (2021) Coke Deactivation and Regeneration of HZSM-5 Zeolite Catalysts in the Oligomerization of 1-Butene, *Applied Catalysis B: Environmental*, 291, 120076, DOI: 10.1016/j.apcatb.2021.120076
- [25] Beirnaert, H.C., Alleman, J.R., Marin, G.B. (2001). A Fundamental Kinetic Model for the Catalytic Cracking of Alkanes on a USY Zeolite in the Presence of Coke Formation, *Ind. Eng. Chem. Res.* 40, 1337–1347. DOI: 10.1021/ie00049